Drug and Chemical Toxicology

ISSN: (Print) (Online) Journal homepage: https://www.tandfonline.com/loi/idct20

Interactive effect of carbendazim and imidacloprid on buffalo bone marrow derived mesenchymal stem cells: oxidative stress, cytotoxicity and genotoxicity

Harpreet Singh, Milindmitra Kashinath Lonare, Manjinder Sharma, Rahul Udehiya, Saloni Singla, Simrat Pal Saini & Vinod Kumar Dumka

To cite this article: Harpreet Singh, Milindmitra Kashinath Lonare, Manjinder Sharma, Rahul Udehiya, Saloni Singla, Simrat Pal Saini & Vinod Kumar Dumka (2021): Interactive effect of carbendazim and imidacloprid on buffalo bone marrow derived mesenchymal stem cells: oxidative stress, cytotoxicity and genotoxicity, Drug and Chemical Toxicology, DOI: 10.1080/01480545.2021.2007023

To link to this article: https://doi.org/10.1080/01480545.2021.2007023

Published online: 29 Nov 2021.

DRUG AND CHEMICAL TOXICOLOGY
https://doi.org/10.1080/01480545.2021.2007023

Taylor & Francis
Taylor & Francis Group

RESEARCH ARTICLE

Interactive effect of carbendazim and imidacloprid on buffalo bone marrow derived mesenchymal stem cells: oxidative stress, cytotoxicity and genotoxicity

Harpreet Singh[a], Milindmitra Kashinath Lonare[a], Manjinder Sharma[b], Rahul Udehiya[c], Saloni Singla[a], Simrat Pal Saini[a] and Vinod Kumar Dumka[a]

[a]Department of Veterinary Pharmacology and Toxicology; [b]Department of Veterinary Physiology and Biochemistry; [c]Department of Veterinary Surgery and Radiology, Guru Angad Dev Veterinary and Animal Sciences University, Ludhiana, Punjab, India

ABSTRACT

The effect of a combination of two pesticides, carbendazim (CBZ) and imidacloprid (IMI), was investigated on mesenchymal stem cells derived from the bone marrow of buffalo (bMSCs). The bMSCs were exposed to the CBZ (2.25 μM, 4.49 μM, and 8.98 μM) and IMI (0.81 mM, 1.61 mM, and 3.22 mM) alone as well as in combinations. The bMSCs were found to be positive for the stem cell markers, AP, CD73, and OCT4. The bMSCs showed a significant reduction ($p \leq 0.05$) in cell viability, and status of anti-oxidants while a significant increase ($p \leq 0.05$) in the level of LDH, ALP, and CK-MB in CBZ and IMI-treated groups. A significant increase ($p \leq 0.05$) was noticed in LPO, O^{2-} radical, total ROS, loss of $\Delta\Psi m$, apoptotic index, and DNA damage in CBZ and IMI-treated groups. A low-dose combination group showed an elevated effect compared to the groups treated with the single pesticide. The interaction index was calculated for CBZ-IMI combined treatment groups on various parameters that showed the majority of antagonist effects. Present findings confirmed that CBZ and IMI-induced cytotoxicity in bMSCs was mediated via ROS production, altered $\Delta\Psi m$ and LPO along with depressed antioxidant status which was responsible for cell apoptosis and cell damage. This study suggested that CBZ and IMI had a dose-dependent toxic effect when the pesticides were used alone, while, co-exposure to both the pesticides simultaneously had an antagonist or non-additive effect on buffalo bMSCs at lower dose combinations and they induced a potentiating effect at high-dose combination.

ARTICLE HISTORY
Received 10 November 2020
Revised 6 May 2021
Accepted 13 May 2021

KEYWORDS
DNA damage; ROS; apoptosis; carbendazim; imidacloprid; interaction index

Introduction

Modern agriculture relies heavily on the use of pesticides to increase food production by controlling pest infestations. Among all the pesticides, insecticides and fungicides are extensively used in agriculture followed by herbicides and rodenticides (Damalas and Koutroubas 2017). Careless and poor techniques for applications of pesticides, adopted by the farmers, resulting in the accumulation of pesticide residues in foodstuffs in amounts above maximum residue levels that may harm plants and animals (Kumar 2004). Imidacloprid (IMI) is a neonicotinoid insecticide used to control sucking insects on plants and as an ectoparasiticide in companion animals (Caron-Beaudoin *et al*. 2017). It produces insecticidal action by acting as an agonist at the insect nicotinic acetylcholine receptors (nAChRs). It has a higher binding affinity for insect nAChRs as compared to mammals, which is responsible for its low mammalian toxicity (Arfat *et al*. 2014). Exposure to IMI may cause damage to the heart, liver, kidney, testis, and other organ systems and may lead to immunotoxicity in non-targeted animal species (Caron-Beaudoin *et al*. 2017, Chakroun *et al*. 2017). Carbendazim (CBZ) is a broad-spectrum benzimidazole fungicide that is commonly applied for plant fungal disease control. The use of CBZ has increased several folds in agricultural practices in recent years and reports have been documented about future consequences of CBZ on the animal testis, sexual maturity, development of the fetus, and hormonal regulation by directly acting on hypothalamic, pituitary, thyroid, and other endocrine glands (Cevik *et al*. 2017, Patil *et al*. 2018). Exposure to pesticides may produce an imbalance between endogenous antioxidants and reactive oxygen species (ROS), with a subsequent decrease in antioxidant defenses to trigger oxidative stress in biological systems, damage to tissues, inflammation, degenerative diseases, aging, and many more diseases (Valavanidis *et al*. 2006, Patil *et al*. 2018).

The application of two or more types of pesticides on crops for a variety of pest control is a common crop cultivation practice throughout the world. Thus, the presence of a mixture of pesticides is common in the environment which results in the persistence of several pesticides in mediums like food, soil, and water from rivers and lakes that support aquatic and other forms of life (Gilliom *et al*. 2006). Therefore, assessing the cumulative toxicity of pesticides in mixtures has been an enduring challenge for researchers involved in environmental science as well as ecotoxicology for many decades. The mixture of pesticides may have a combined deleterious influence on plants and animals,

CONTACT Milindmitra Kashinath Lonare milindmitra@gmail.com Department of Veterinary Pharmacology and Toxicology, Guru Angad Dev Veterinary and Animal Sciences University, Ludhiana-141 004 Punjab, India

ranging from beneficial soil microorganisms and insects to non-target plants, livestock, fish, birds, and wildlife (Bind and Kumar 2019). The presence of two or more pesticides in the body may influence the toxicological effects of each other in various ways depending upon the properties of the individual compounds and their chemical classes, dose and the targeted organs leading to variation in toxic effects that can be determined by toxicokinetic-dynamic factors involved in the metabolic pathways and molecular targets of individual pesticides. The pesticide mixture may lead to unpredictable toxic effects such as potentiation, synergism, or antagonism (Hernández *et al*. 2017).

Buffalo forms the backbone of the Indian dairy industry and is reared widely by small farmers as well as organized dairy farms. Thus, it has an enormous contribution to the national GDP. Despite that research focus on buffaloes is still lacking as compared to any other animal species. The bone marrow-derived buffalo mesenchymal stem cells (bMSCs) represent a promising tool for the development of *in vitro* assay model that may improve or replace the current predictive toxicological research on cell culture of the target species. The biological responses elicited by the interaction of toxicants with different chemicals in nature may be studied using a toxicological approach with this model system. Moreover, bMSCs have not been adopted yet as an *in vitro* model system for toxicity testing of environmental toxicants. In view of the paucity of data on the toxic effects of simultaneous exposure of CBZ and IMI on bMSCs, the study was planned to evaluate the effects of CBZ and IMI alone as well as in combination on bMSCs.

Materials and methods

Chemicals and reagents

Technical grade carbendazim, RBC lysis buffer, Hoechst-33258, and Histopaque-1077 were procured from Sigma Aldrich, USA, and imidacloprid from M/s Gharda Chemicals, Pvt. Ltd. Mumbai. Goat Polyclonal IgG primary antibodies against CD73 and OCT4; and secondary antibodies conjugated with FITC (Donkey Antigoat IgG-FITC) and TexasRed (Donkey antigoat IgG-TR) against primary antibody were procured from Santa Cruz Biotechnology, Inc., California. Chemicals of analytical grade, kits, and enzymes used in the present study were obtained from established firms such as Sigma, Bangalore-Genei, Himedia, Merck, SD Fine Chemicals, Span Diagnostics, and ERBA Diagnostics Pvt. Ltd.

Stock solution and growth medium

Stock solutions of 2 M IMI (510.2 *g* L^{-1}) and 0.5 M CBZ (95.6 *g* L^{-1}) were prepared in DMSO. The growth medium was prepared by adding 15% fetal bovine serum (FBS) and antibiotics in Dulbecco's Modified Eagle's Medium (DMEM) for culturing bMSCs. Phosphate buffer saline (PBS; pH 7.4) was prepared with milli-Q water, autoclaved, and stored at 4 °C till use.

Collection, isolation and culturing of bMSCs

Bone marrow samples were aspirated from the iliac crest of the pelvis from buffalo calves immediately after stunning under sterile conditions using a sterile Jamshidi needle (11 G) with 20-ml syringes containing 250 units of heparin. Immediately after the collection bone marrow samples were transported to the laboratory for further processing. A mixed population of stem cells was isolated by density gradient method with Histopaque-1077 in a ratio 1:1 in 15 ml centrifuge tubes and centrifuged at 2500 rpm for 25 minutes at room temperature. After centrifugation, the mononuclear cell suspension was visible as a buffy coat consisting of a mixed population of cells (lymphocytes and stem cells). The suspension was carefully transferred to another 15 ml centrifuge tube and washed with PBS thrice followed by treatment with RBC lysis buffer at room temperature for 5 minutes. The resultant cell pellet was suspended in a growth medium and incubated with 5% CO_2 at 37 °C temperature. Culture flasks were kept undisturbed for cell attachment and after 72 h of cell attachment, the suspended cells were removed along with the medium and replaced with a fresh growth medium. After reaching 80–90% cell confluency, bMSCs were subjected to trypsinization for sub-culturing (Figure 1). Cells after the third passage with uniform cell populations were used for the characterization and other toxicological assessments.

Characterization of mesenchymal stem cells

The bMSCs were characterized after the third passage with alkaline phosphatase (AP) staining. Cells were seeded into a culture dish provided with a complete growth medium and allowed to grow up to 70–80% of confluency. Thereafter, growth media was decanted. The cells were fixed with 4% paraformaldehyde for 2 minutes followed by washing with PBS three times. Then the bMSCs were incubated with 25 mM Tris-HCl and 150 mM NaCl containing 8 mM $MgCl_2$, 0.4 mg/ml Naphthol AS-MX phosphate and 1 mg/ml Fast Red TR salt for 1 hr at 37 °C. Finally, cells were washed with PBS and visualized under a bright and fluorescent microscope (Gade *et al*. 2012, Devi *et al*. 2017).

CD73 and OCT4 stem cell markers, specific to bMSCs, were characterized by immunostaining after achieving 70–80% cell confluency. The bMSCs were washed thoroughly with PBS thrice after removing the medium and were fixed in 4% formalin solution prepared in PBS for 10 minutes at 37 °C. Antigen retrieval was done with sodium citrate in PBS for 20 minutes at 37 °C. Nonspecific bindings were blocked by incubating the cells with donkey serum (1:10 dilution in PBS) for 30 minutes at 37 °C. The bMSCs were then incubated with primary antibodies (1:50 dilution in PBS) for 1 h at 37 °C followed by incubation with secondary antibodies (1:200 dilution in PBS) and conjugated with FITC and/or Texas Red for 1 h at 37 °C. The staining procedure for negative control cells was also performed in a similar manner to that of positive controls with the exception that the primary antibody was skipped to check the nonspecific binding of the secondary antibodies in the negative control cells. Each step was followed by washing with PBS three times. The stained bMSCs

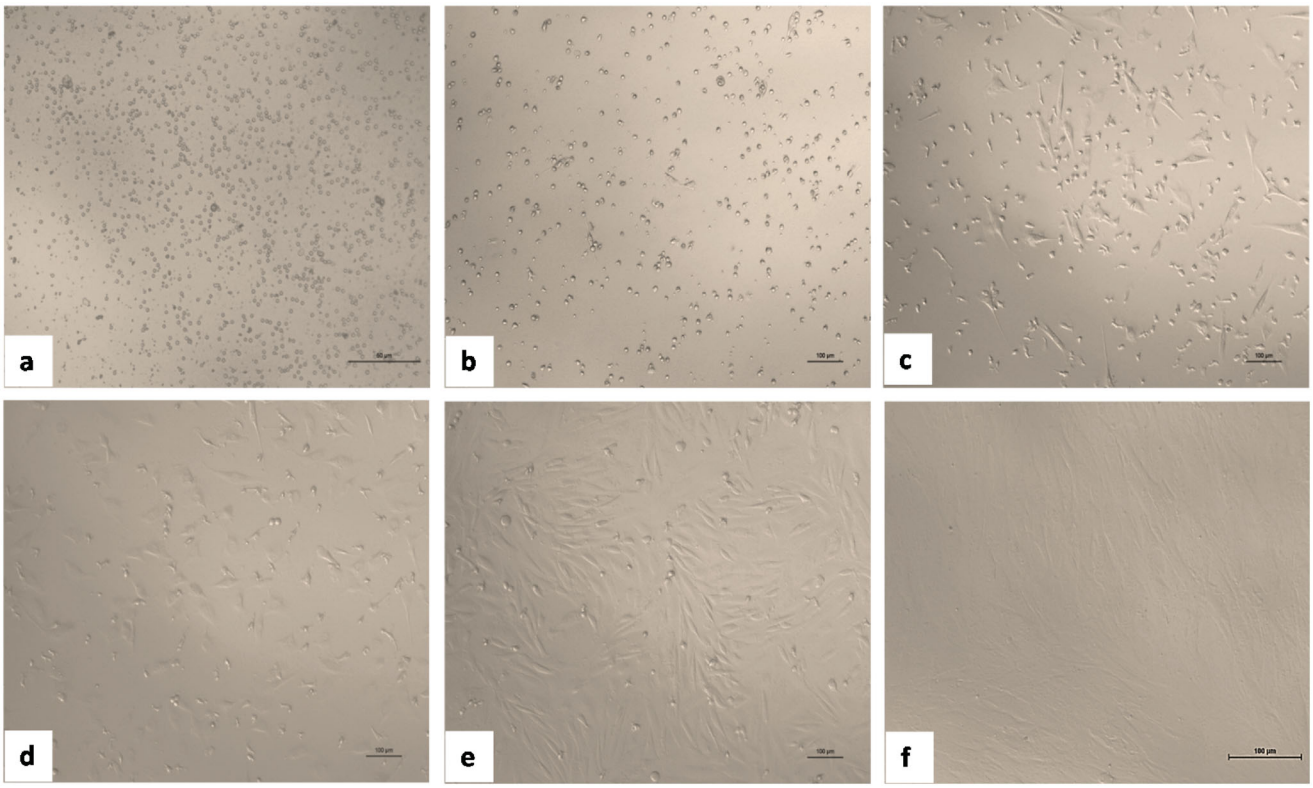

Figure 1. Isolation and culture development of bone marrow derived buffalo mesenchymal stem cells at different time and passages. (a) day 0; (b) day 3; (c) day 9; (d) day 12; (e) day 21; and (f) day 28 confluent monolayer (Original magnification: (a): X40; (b,f): X20; (c,d,e): X10).

were observed under a fluorescent microscope with the filters of a specific wavelength (Gade *et al*. 2012, Devi *et al*. 2017).

Determination of inhibitory concentration

Repeated pilot experiments were conducted to establish the dose range CBZ and IMI on bMSCs. The final working solutions of CBZ and IMI were prepared in a complete growth medium ranging from 0.254 to 5.00 mM and 0.0106 to 400.00 mM, respectively. Previously published population doubling time (PDT) of bMSCs was referred (Gade et al. 2012, Devi *et al*. 2017) and PDT of bMSCs for the present study was calculated (39.20 ± 0.81 h). A comparison of PDT was made and 48 h exposure time was selected. The bMSCs were exposed to these concentrations of pesticides for a period of 48 h. After completion of the exposure period, the cell viability assay/MTT assay was performed to calculate the inhibitory concentration (IC_{50}). A log dose-response curve was plotted for the determination of IC_{50}. Further, IC_{25}, $IC_{12.5}$, and $IC_{6.25}$ concentrations were calculated for CBZ and IMI.

Cell viability assay

The bMSCs were grown in a growth medium and incubated with 5% CO_2 at 37^0 C temperature in the presence of various concentrations of CBZ and IMI. At the end of the exposure period, MTT (3–(4,5-dimethylthiazol-2-yl)-2,5-diphenyl tetrazolium bromide) assay was performed according to the standard procedure (Bahuguna *et al*. 2017). The MTT assay is based on the conversion of yellow MTT formazan crystals to the purple end-product, formazan, by the solubilizing medium (DMSO). The assay was optimized for the bMSCs culture and used in this study. Cells were seeded in a 96-well cell culture plate at a density of 6×10^3 cells/well and allowed to grow for 12 h by providing all culture conditions. The bMSCs were exposed to different concentration range of 0.254, 0.7621, 2.286, 6.859, 20.576, 61.728, 185.185, 555.556, 1666.667 and 5000.00 μM for CBZ and 0.010, 0.030, 0.091, 0.274, 0.823, 2.469, 7.407, 22.222, 66.667 and 200.000 mM for IMI for 48 h. Control bMSCs exposed to 1% DMSO served as vehicle control, while cells without any treatment served as control. Finally, after the completion of 48 h of the exposure period, the medium was removed and cells were incubated for 3 h with 20 μL (5 mg/mL) MTT solution in DMEM, without phenol red at 37 °C in 5% CO_2 humidified chamber. On completion of the incubation period, formazan was solubilized in DMSO with gentle intermittent shaking for 20–30 minutes inside the incubator, in the dark, until complete dissolution was achieved. The plates were read at 570 nm (test wavelength) and 720 nm (reference wavelength) using the Tecan Infinite M200 Multiplate Reader (Tecan Austria).

The absorbance values and all results were presented as a percentage of the control values (viability/control; % of cell survival). The percentage of cell survival was expressed with the following formula and IC_{50} of the CBZ and IMI were calculated.

$$\% \text{ of cell survival} = [\text{Absorbance tested compound}/\text{Absorbance control}] \times 100$$

$$IC_{50} = 100 - \% \text{ of cell survival}$$

Experimental design

IC_{25}, $IC_{12.5}$, and $IC_{2.25}$ values of CBZ and IMI were derived from IC_{50} values. The bMSCs were exposed to the CBZ (2.25, 4.49, and 8.98 μM) and IMI (0.81, 1.61, and 3.22 mM) alone and in four different combinations of CBZ (2.25 and 4.49 μM) and IMI (0.81 and 1.61 mM). Cells from the control group were provided with a normal basal growth medium and the vehicle control group was exposed to 1% DMSO in a growth medium for 48 h. Toxicity end parameters were evaluated after completion of the exposure period (Table 1) along with cell viability assay/MTT assay by the method of Bahuguna *et al*. (2017) as described earlier.

Assessment of biochemical parameters

The biochemical parameters were estimated in the cell culture medium at the end of the exposure period and the medium was stored at −20 °C till analysis. Estimation of lactate dehydrogenase (LDH), alkaline phosphatase (ALP), creatine-kinase (CK) and gamma-glutamyl transferase (GGT) were performed using commercial kits (ERBA Diagnostics, Mannheim GmbH, manufactured by Transasia Bio-Medicals Ltd. Mumbai, India).

Estimation of oxidative stress indicators and antioxidant enzymes

The oxidative stress and antioxidant parameters were estimated in cell lysate at the end of the exposure period and the cell lysate was stored at −20 °C until analysis. Cell lysis buffer comprised of 30 ml of 150 mM NaCl, 10 ml of 5 mM EDTA, 50 ml of 50 mM Tris-HCl, 10 ml of 0.1% Triton X-100, 10 ml of 0.1% SDS and 10 ml of 0.1% glycerol. The final volume was made to 1 liter with distilled water and pH was adjusted to 8.0. Ice-chilled cell lysis buffer was added to the cell culture plate for 10 minutes and thereafter the lysate was collected and preserved at −20 °C.

Table 1. Experimental design showing treatment of CBZ and IMI alone and in combinations with an exposure period of 48 h.

Group	Treatment	Dose
I	Control	–
II	DMSO	1%
III	CBZ-I	2.25 μM
IV	CBZ-II	4.49 μM
V	CBZ-III	8.98 μM
VI	IMI-I	0.81mM
VII	IMI- II	1.61 mM
VIII	IMI- III	3.22 mM
IX	CBZ-I + IMI- I	2.25 μM + 0.81 mM
X	CBZ-I + IMI- II	2.25 μM + 1.61 mM
XI	CBZ-II + IMI- I	4.49 μM + 0.81 mM
XII	CBZ- II + IMI- II	4.49 μM + 1.61 mM

*All experiments were performed in duplicate with three replicate each.
Where; CBZ: Carbendazim and IMI: Imidacloprid; DMSO: Dimethyl-sulphoxide.
bMSCs were exposed to different concentrations of CBZ (2.25, 4.49, and 8.98 μM) and IMI (0.81, 1.61, and 3.22 mM) alone and four combinations of CBZ (2.25 and 4.49 μM) and IMI (0.81 and 1.61 mM). bMSCs from the control group were provided with a basal growth medium and vehicle control provided 0.1% DMSO in a basal growth medium. Cell viability assay/MTT assay performed by standard procedure with completion of exposure (Bahuguna et al. 2017).

Spectrophotometric methods were used for measurement of the lipid peroxidation (LPO) (Stocks and Dormandy 1971), O_2^- radical generation (Wang 2000), GSH content (Beutler & Kelly 1963), and total protein content (Lowry *et al*. 1951). The activity of antioxidant enzymes SOD (Madesh & Balasubramanian 1998), GST (Habig *et al*. 1974), GPx (Hafeman *et al*. 1974), and CAT (Aebi 1984) were assayed by the standard spectrophotometric methods.

ROS and ΔΨm/MTP measurement

The 2,7-dichlorofluorescin diacetate (DcFHDA) assay was used to estimate total ROS (hydroxyl, peroxyl and other ROS) activity within the cells (Aranda *et al*. 2013). The 3,3-dihexyloxacarbocyanine iodide [$DiOC_6(3)$] labels the mitochondria and is used to estimate the change in mitochondrial transmembrane potential (MTP/ΔΨm) in the cells which is associated with a reduction of $DiOC_6(3)$ uptake (Salmon 2013).

A stock solution of 2 mM DCFHDA (working solution 20 μM) and 1 mM $DiOC_6$ (working solution 10 μM) was prepared. Required final working solutions were prepared and used for measurement of ROS production and change in ΔΨm in adherent cell culture 48 h post-exposure. Cells were observed under the fluorescent microscope (Nikon DSRi1, Japan) with a requisite wavelength (excitation 482 nm and emission 500 nm for ΔΨm; excitation 520 nm and emission 550 nm for ROS). Percent of cells positive for ROS production (Figure 2) and loss of ΔΨm (Figure 3) were calculated after counting 500 cells from each group.

Determination of apoptosis

Acridine orange/Ethidium bromide (AO/EB) staining was used to determine the morphological changes in nuclei structures, reflecting the apoptotic insults (Baskić et al. 2006). Various apoptotic parameters were calculated using standard formulae.

$$\text{Per cent of apoptotic index} = (V_A + NV_A)/(V_N + V_A + NV_N + NV_A) \times 100$$

$$\text{Per cent of necrotic cells} = (NV_N/V_N + V_A + NV_N + NV_A) \times 100$$

$$\text{Per cent of dead cells} = (NV_N + NV_A/V_N + V_A + NV_N + NV_A) \times 100$$

where, V_N: Viable cells with normal nuclei, V_A: Viable cells with apoptotic nuclei, NV_N: Non-viable cells with normal nuclei and NV_A: Non-viable cells with apoptotic nuclei.

Alkaline comet assay

The alkaline comet assay/single cell gel electrophoresis (SCGE) was performed according to procedures described by previous researchers (Tice *et al*. 2000). Briefly, bMSCs were seeded in 24 well plates and harvested at the end of the exposure period of 48 h. The frosted end slides were coated with a thin layer of 1% normal-melting-point agarose (NMA). Slides were stored at room temperature in a dust-free and

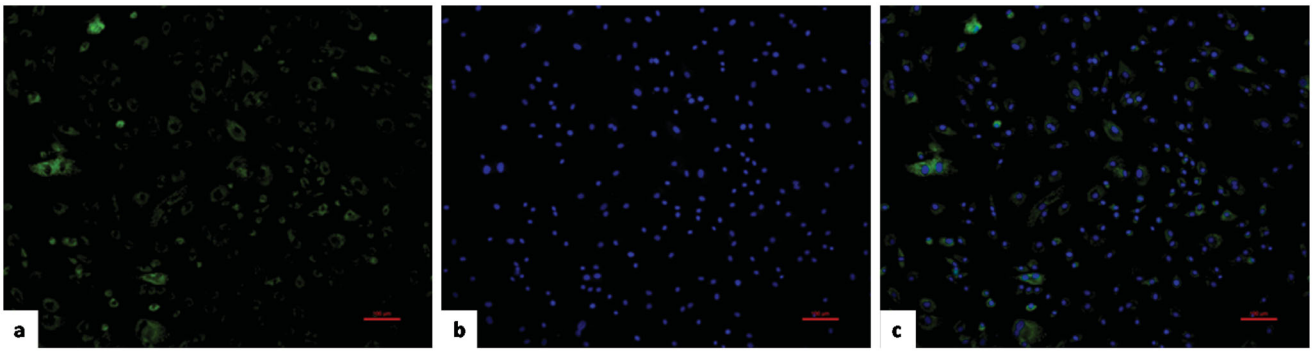

Figure 2. Photomicrographs from representative bMSCs showing ROS measurement using fluorescence microscopy. (a) Cells with green fluorescence indicating intracellular DCF formation (ROS positive); (b) blue fluorescence indicating nuclear staining (Hoechst), while, (c) dual fluorescence staining. (Original magnification: (a–c): X10).

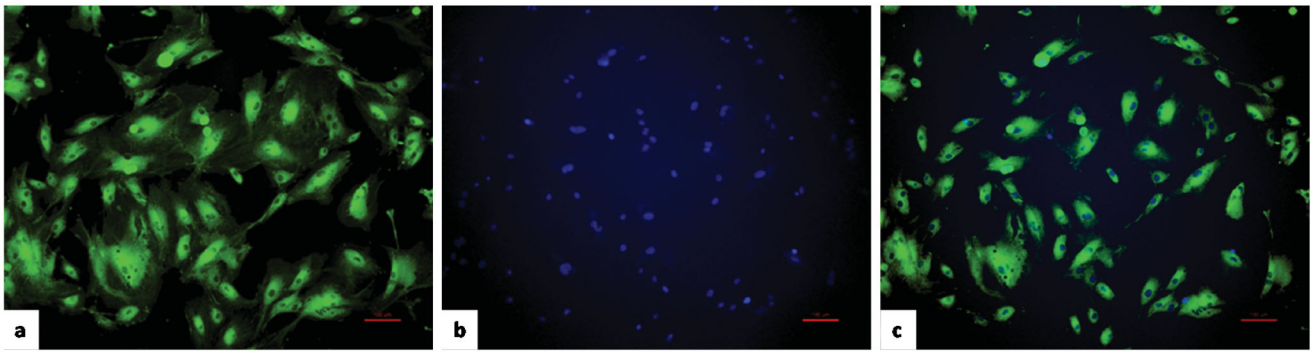

Figure 3. Photomicrographs from representative bMSCs showing $\Delta\Psi$m in fluorescence microscopy with $DiOC_6$ uptake assay. (a) Green fluorescence indicating intracellular $DiOC_6$ uptake by the cells with normal $\Delta\Psi$m, (b) fluorescence indicating nuclear staining (Hoechst), while, (c) dual fluorescence staining (Original magnification: (a–c): X10).

dry environment. 100 µl of 1% low-melting-point agarose (LMPA) was mixed gently with 10 µl of bMSCs, then 80 µl of suspension was layered on the base slide in two replicates, and coverslips were placed on it. The slides were kept at 4 °C for 5–10 minutes until agarose got solidified. After solidification of agarose, coverslips were taken off and 80 µl of 0.5% LMPA was added to the slides. Coverslips were replaced and slides were again put on an ice pack for solidification. The coverslips were then carefully removed and the slides were immersed for 20 minutes in a Coplin staining jar containing freshly prepared alkaline buffer (2.5 M NaCl, 100 mM EDTA, 10 mM Trisma base, 8 *g* NaOH, 1 ml Triton X-100 and 10 ml DMSO with final volume made 100 ml with distilled water, pH = 10) at 4 °C for 1 h. The slides were placed in a horizontal electrophoresis chamber (Genei System Inc.) containing freshly prepared cold electrophoresis alkaline buffer (300 mM NaOH, 1 mM EDTA, pH $\geq$ 13) for approximately 25 minutes to unwind the DNA. Electrophoresis was carried out at 24 V with 300 mA for 20–30 minutes in the dark. Slides were gently lifted and placed on a dry tray, flooded with freshly prepared neutralization buffer (0.4 M Tris, pH 7.5) for 5 minutes. The slides were then washed with freshly prepared neutralization buffer for 5 minutes, fixed with cold absolute methanol for 5 minutes, and air-dried at room temperature. Further, 50 µL of ethidium-bromide (20 mg/mL) was added to each slide to stain the DNA and the slides were examined under a fluorescent microscope (Nikon DSRi1, Japan) with an excitation filter (515–560 nm) and a barrier filter (590 nm). To visualize DNA damage, slides were observed at 20X magnification using a micrometric eyepiece/objective combination. Genotoxicity was evaluated using ImageJ (NIH) image analysis software based on comet tail length, tail DNA percent, olive moment, and tail moment.

Joint action analysis

The interaction index (I.I.) or combinational index (C.I.) was calculated for the different biochemical parameters to see the types of effect as per the standard formula (Mansour and Refaie 2000) to identify the type of interaction between pair of toxicants which was termed as interaction index (I.I.).

$$\text{I.I.} = \text{M} + \text{C}/\text{A1} + \text{A2}$$

where; M, C, A1 & A2 represent the mean values obtained from the estimated studied parameter. M: the value of the mixture or combination-treated group, A_1 and A_2: values of the groups treated with a single pesticide, C: the value of the control group. Based on the I.I. formula, the ratings of the interaction indices are interpreted as bellow;

In case of positive effect (i.e., increase in the concerned biochemical parameters above the control values due to effect of the individual compounds), I.I.>1 means potentiation; I.I.=1 means additive; I.I.<1 means antagonism. In case of a negative effect (i.e., decrease in the concerned biochemical parameters below the control values due to the effect of the individual compounds), I.I.>1 means antagonism; I.I.=1 means additive; I.I.<1 means potentiation.

Statistical analysis

The data were subjected to statistical analysis using IBM SPSS Statistics software and Microsoft Excel. All the data were compared by employing One-Way Analysis of Variance (ANOVA) with Tukey's multiple comparisons as a *post hoc* test. All the data were expressed as Mean ± SEM. A p values of <0.05 was considered statistically significant.

Results

Characterization of bMSCs

Alkaline phosphatase activity was detected positive in bMSCs and cells appeared red after staining (Figure 4: a-b). A polyclonal antibody specific to bMSCs against CD73 and OCT4 were used to characterize the bMSCs progenitor and pluripotency. These stem cell markers showed positive expression

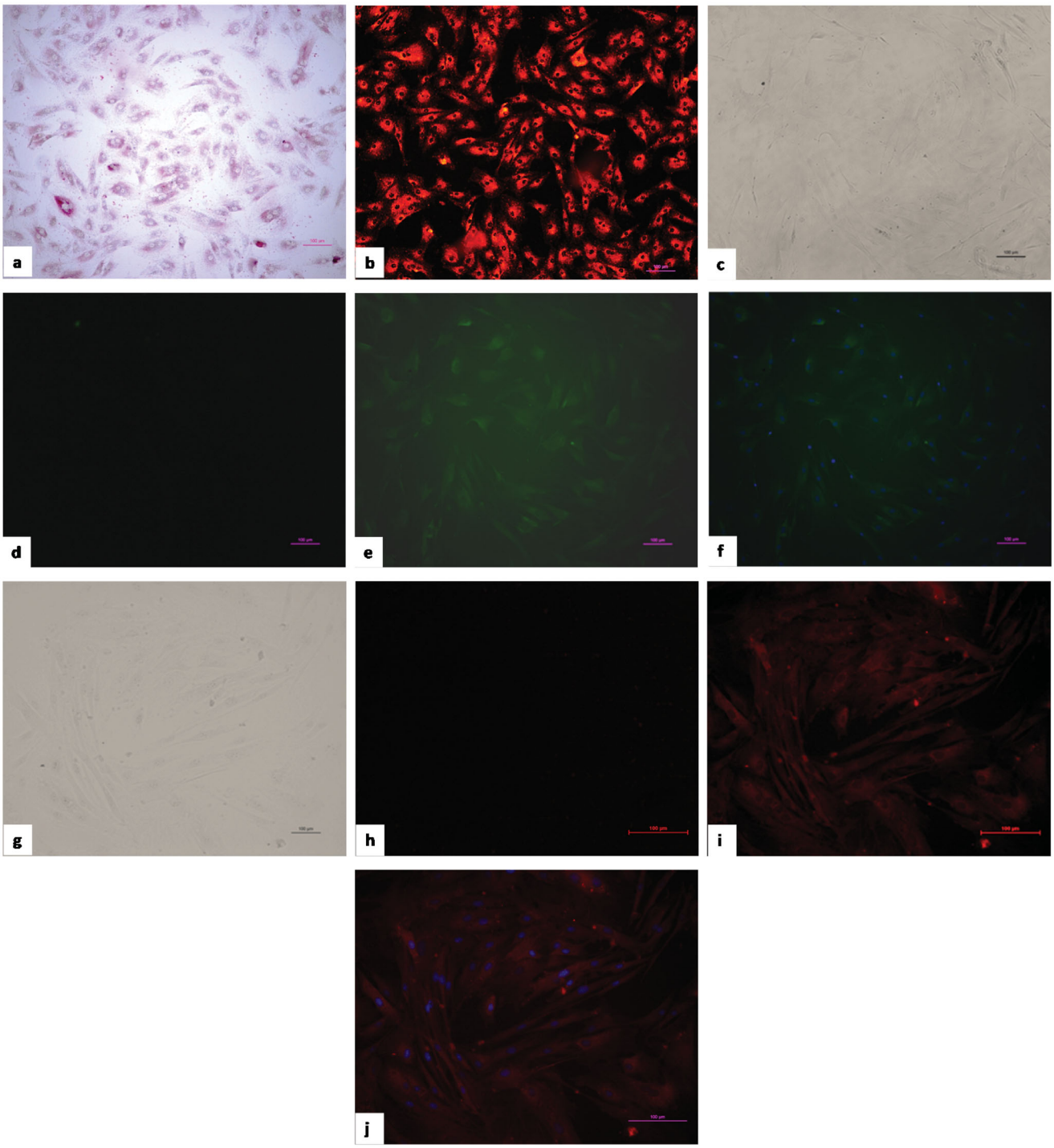

Figure 4. Photomicrographs of bMSCs showing alkaline phosphatase staining under (a) bright field and (b) fluorescent field. Buffalo bMSCs showing immunofluorescent staining for localization of CD73 (c–f) and OCT4 (g–j) with FITC or Texas Red-conjugated with secondary antibodies, respectively. Where; (c,g) under bright field, (d,h) control negative, (e,i) FITC or Texas Red-conjugated with secondary antibodies, (f,j) dual fluorescence staining, blue fluorescence indicating nuclear staining (Original magnification: (a–j): X10).

for CD73 and OCT4 as revealed by green and red fluorescence, respectively (Figure 4: c-f).

Effect on inhibitory concentration

CBZ exhibited cytotoxic activity with IC_{50} value 17.97 µM (Figure 5a). Further, IC_{25}, $IC_{12.5}$, and $IC_{6.25}$ were calculated to be 8.98, 4.49, and 2.25 µM, respectively. IMI exhibited IC_{50} value of 6.446 mM (Figure 5b). Further, IC_{25}, $IC_{12.5}$, and $IC_{6.25}$ were calculated to be 3.22, 1.61, and 0.81 mM, respectively.

Effect on cell viability

Cell viability was found to be lowest in group XII (CBZ-II + IMI-II) and was comparable to group V (high-dose CBZ alone). Viability percent significantly decreased ($p < 0.05$) from group III to group V and from group VI to group VIII with increasing doses of CBZ and IMI, respectively, in a dose-dependent manner, in comparison to the control group (Figure 6a). Viability percent values were found to be significantly higher ($p < 0.05$) in CBZ-I and CBZ-II treatments as compared to IMI-I and IMI-II treatment groups.

Effect on biochemical parameters

A non-significant increase ($p > 0.05$) in LDH and GGT activity with increasing concentrations of CBZ and IMI alone and the combination-treated groups was noticed as compared to the control group (Figure 6b; Table 2). A significant increase ($p < 0.05$) in the activity of CK-MB and ALP with increasing concentrations of CBZ and IMI treatments was observed when compared to the control group (Table 2). Significantly higher ($p < 0.05$) ALP activity was noticed in co-treated groups (XI and XII groups) as compared to the control group. ALP activity was found to be significantly different ($p > 0.05$) between CBZ-II and IMI-II alone treatment groups. CK-MB activity in CBZ alone treatments was significantly higher ($p < 0.05$) than the IMI-II and IMI-III alone treatment groups.

Effects on the antioxidant system

A significant decrease ($p < 0.05$) in SOD, CAT, GPx, and GST activity was observed in CBZ, IMI alone and in the co-treated groups when compared with the control group. Very low activity was noticed in CBZ-III group and CBZ-II + IMI-II group (Table 3). However, a non-significant change ($p > 0.05$) in GSH content was noticed in alone and co-treated groups as compared to the control group. GPx activity was significantly different between all CBZ and IMI alone treatment groups except for CBZ-II and IMI-II groups. A significant difference was observed between all CBZ and IMI alone treatments except in CBZ-I and IMI-II groups for SOD activity. IMI-II alone treatment group showed a significant change ($p < 0.05$) in

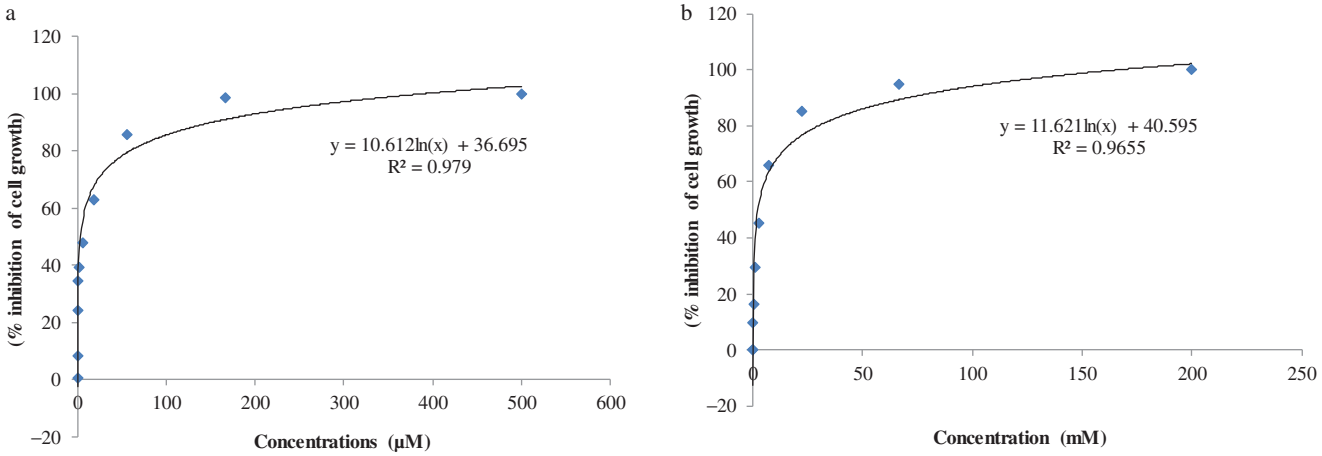

Figure 5. Graph showing the log-dose response curve of bMSCs. Concentrations vs. percent cell inhibition (a) CBZ and (b) IMI. CBZ: imidacloprid; IMI: imidacloprid.

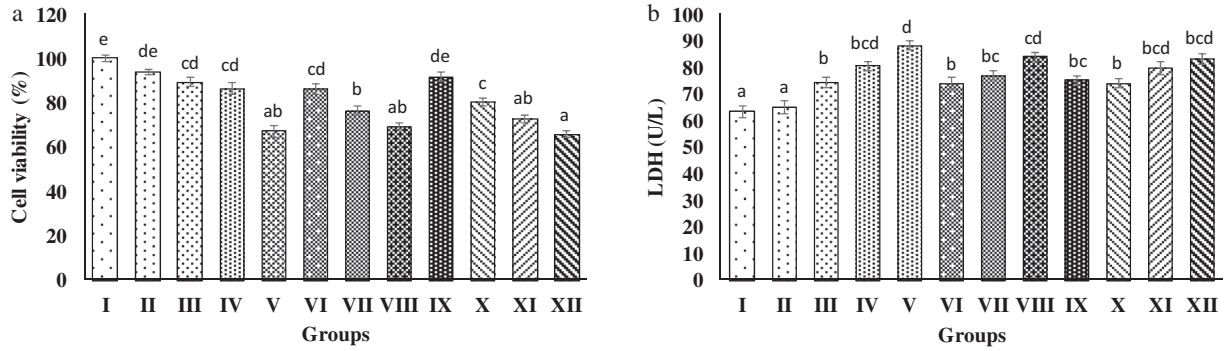

Figure 6. Effect of CBZ and IMI in alone or in combinations on (a) cell viability and (b) LDH activity 48 h of post exposure on bMSCs. Each column represents Mean ± SEM ($n = 6$), different superscripts differ significantly from each other. ($p \leq 0.05$) in One-way ANOVA with Tukey's multiple comparison *post hoc* test. CBZ: carbendazim, IMI: imidacloprid, LDH: lactate dehydrogenase.

Table 2. Effect of CBZ and IMI alone and in combinations on antioxidant enzymes and non-enzyme system 48 h of post-exposure on bMSCs.

Groups	GSH	SOD	CAT	GPx	GST
I	6.87 ± 0.39^{b}	0.418 ± 0.000^{b}	4.15 ± 0.28^{a}	10.41 ± 0.27^{a}	0.0223 ± 0.00051^{d}
II	7.06 ± 0.41^{b}	0.379 ± 0.010^{c}	3.93 ± 0.24^{b}	9.04 ± 0.15^{b}	0.0228 ± 0.0003^{c}
III	6.67 ± 0.22^{b}	0.380 ± 0.007^{c}	3.70 ± 0.19^{b}	8.62 ± 0.11^{b}	0.0240 ± 0.0003^{a}
IV	6.52 ± 0.28^{b}	0.285 ± 0.004^{d}	3.15 ± 0.09^{d}	2.91 ± 0.08^{f}	0.0201 ± 0.0003^{f}
V	6.79 ± 0.25^{b}	0.169 ± 0.003^{g}	2.38 ± 0.14^{d}	0.10 ± 0.00^{i}	0.0174 ± 0.0001^{g}
VI	6.68 ± 0.31^{b}	0.447 ± 0.008^{a}	3.65 ± 0.28^{b}	6.92 ± 0.17^{d}	0.0245 ± 0.0006^{a}
VII	7.41 ± 0.32^{a}	0.355 ± 0.007^{c}	3.21 ± 0.24^{c}	2.85 ± 0.08^{f}	0.0212 ± 0.0002^{e}
VIII	6.99 ± 0.03^{b}	0.241 ± 0.004^{e}	2.51 ± 0.12^{d}	0.94 ± 0.04^{h}	0.0175 ± 0.0000^{g}
IX	6.38 ± 0.30^{b}	0.467 ± 0.009^{a}	4.09 ± 0.38^{a}	7.91 ± 0.16^{c}	0.0239 ± 0.0004^{b}
X	6.66 ± 0.19^{b}	0.373 ± 0.008^{c}	3.74 ± 0.30^{b}	5.67 ± 0.31^{e}	0.0211 ± 0.0000^{e}
XI	6.79 ± 0.23^{b}	0.287 ± 0.018^{d}	3.31 ± 0.34^{b}	2.19 ± 0.12^{g}	0.0195 ± 0.0006^{f}
XII	7.00 ± 0.15^{b}	0.197 ± 0.005^{f}	2.48 ± 0.19^{d}	0.64 ± 0.08^{h}	0.0160 ± 0.0002^{h}

Each column represents Mean ± SEM ($n = 6$), different superscripts differ significantly from each other. ($p \leq 0.05$) in One-way ANOVA with Tukey's multiple comparison *post hoc* test. CBZ: carbendazim, IMI: imidacloprid,GSH: glutathione reduced (nmol of GSH/mg of protein); SOD: superoxide dismutase (Units/mg protein);CAT: catalase (nM H_2O_2 utilized/min/mg protein); GPx: glutathione peroxidise (μM NADPH oxidized to NADP/min/mg protein); GST: glutathione S-transferase (μmol/h/mg protein).

Table 3. Effect of CBZ and IMI alone or in combinations on enzymes system of toxicological importance after 48 h of exposure period on bMSCs.

Group	ALP	GGT	CK-MB
I	6.71 ± 0.09^{d}	2.75 ± 0.17^{a}	6.06 ± 0.87^{c}
II	7.35 ± 0.26^{c}	2.88 ± 0.15^{a}	6.70 ± 0.77^{c}
III	6.54 ± 0.18^{d}	2.83 ± 0.23^{a}	5.22 ± 1.02^{c}
IV	7.05 ± 0.17^{d}	2.98 ± 0.25^{a}	5.92 ± 1.68^{c}
V	8.36 ± 0.28^{a}	3.38 ± 0.45^{a}	6.82 ± 0.61^{c}
VI	6.75 ± 0.22^{d}	2.81 ± 0.21^{a}	6.96 ± 1.46^{c}
VII	7.61 ± 0.16^{b}	3.01 ± 0.27^{a}	11.07 ± 1.85^{b}
VIII	8.31 ± 0.37^{a}	3.26 ± 0.38^{a}	15.88 ± 1.63^{a}
IX	6.63 ± 0.21^{d}	2.73 ± 0.25^{a}	5.36 ± 1.03^{c}
X	6.91 ± 0.37^{d}	2.87 ± 0.23^{a}	5.92 ± 0.93^{c}
XI	7.35 ± 0.13^{c}	2.96 ± 0.25^{a}	7.45 ± 1.14^{c}
XII	8.36 ± 0.10^{a}	3.30 ± 0.370^{a}	13.79 ± 2.28^{b}

Each column represents Mean ± SEM ($n = 6$), different superscripts differ significantly from each other. ($p \leq 0.05$) in One-way ANOVA with Tukey's multiple comparison *post hoc* test.CBZ: carbendazim, IMI: imidacloprid; ALP: Alkaline phosphatase (IU/L), GGT: Gamma-glutamyl transferase (U/L), CKMB: creatine phosphate (U/L).

the activity of CAT and GST as compared to all other CBZ alone treatments.

Effects on oxidative stress markers

The total protein content of CBZ and IMI combination-treated groups was found to be quite similar to the respective alone higher-dose treated groups (Figure 7d). A significant difference ($p < 0.05$) in total protein content was noticed between CBZ and IMI alone treatment groups. A significant increase ($p < 0.05$) in the LPO was noticed in CBZ and IMI alone treatment groups when compared to the control group, while, CBZ alone treatments showed significant change ($p < 0.05$) in LPO as compared to the IMI-III alone treatment. The highest LPO was noticed in CBZ-II and IMI-II combined groups (Figure 6a). The bMSCs, when exposed to CBZ and IMI alone and in combinations, caused an increase ($p < 0.05$) in the level of O_2^- radical in comparison to the non-treated bMSCs (Figure 7b). Significantly very high ($p < 0.05$) O_2^- radical level was noticed in CBZ-III treated group followed by CBZ-II + IMI-II-treated group. O_2^- radical levels were significantly different from each other in CBZ and IMI alone treated groups except CBZ-I and IMI-II groups. Further, a significant increase ($p < 0.05$) in ROS generation in a dose-dependent manner was noticed in the CBZ and IMI-treated groups. A significant difference ($p < 0.05$) in ROS generation was noticed between CBZ and IMI alone treatment groups except CBZ-I and IMI-I groups. Maximum numbers of bMSCs positive with ROS were found in the high dose CBZ-treated group as compared to the high dose of IMI treated group (Figure 7c).

Effect on mitochondrial transmembrane potential

A dose-dependent increase in the cells with loss of $\Delta\Psi m$ in CBZ and IMI-treated groups was measured. Co-treated groups showed a significant decrease ($p < 0.05$) in cells with a loss of $\Delta\Psi m$ as compared to the control group but were comparable to single pesticide-treated groups (Figure 7d). $\Delta\Psi m$ was significantly different ($p < 0.05$) from each other in CBZ and IMI alone treatment groups except CBZ-I and IMI-I groups.

Effect on bMSCs apoptosis

Percentage apoptotic index was consistently higher ($p < 0.05$) with increasing dose of CBZ and IMI alone groups as well as for the co-treatment groups in comparison to the control group. A significant increase ($p < 0.05$) in percent necrotic cells and percent dead cells were noticed in CBZ and IMI-exposed groups when compared with the control group (Figure 8a–c). A dose-dependent significant change ($p < 0.05$) in apoptotic index and percent necrotic cells was noticed between CBZ and IMI alone treatment groups except for CBZ-III and IMI-III groups. CBZ-II + IMI-II co-treatment group was found to be more toxic as indicated by an increase in the percentage of necrotic and dead cells.

Effect on bMSCs DNA

Exposure of CBZ and IMI alone caused a significant change ($p < 0.05$) in comet score in terms of comet tail length, tail DNA percent, tail moment, and the olive tail moment when compared with the control group in a dose-dependent manner (Figure 9). The highest significant ($p < 0.05$) olive moment was noticed in CBZ-III treated group when compared to all other groups. Low dose CBZ and IMI combination groups showed a significant change ($p < 0.05$) in DNA damage as

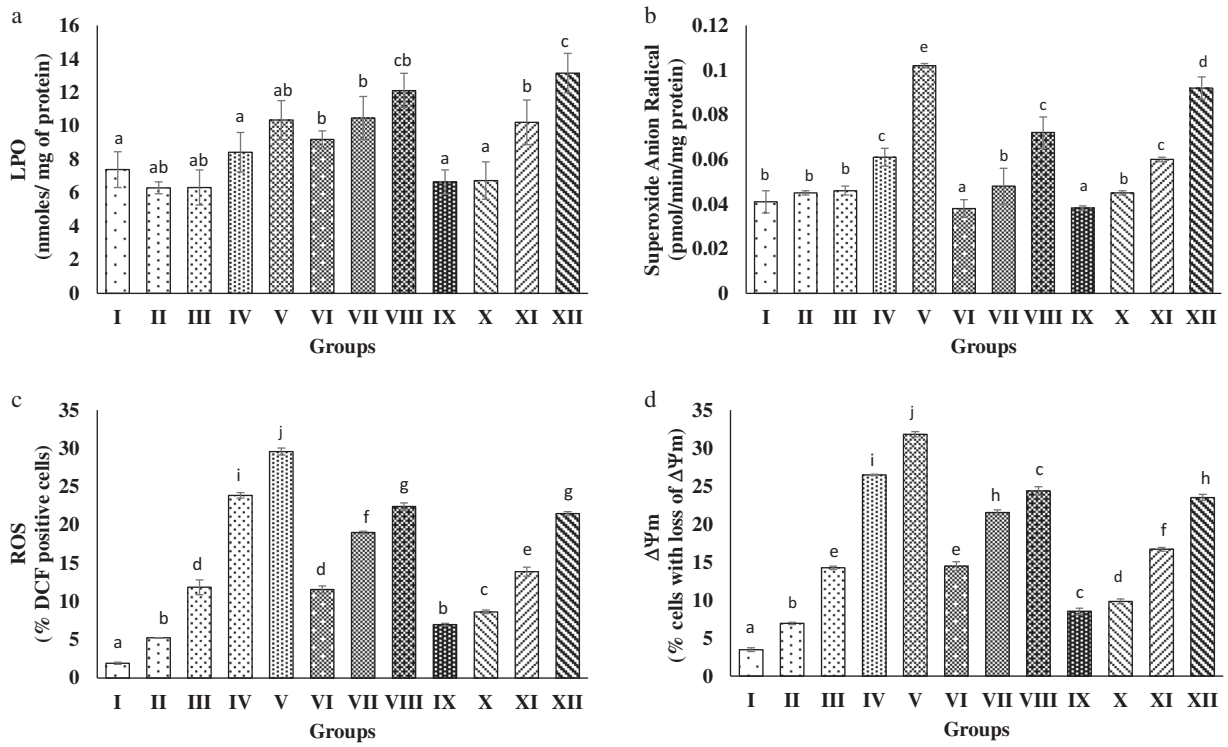

Figure 7. Effect of CBZ and IMI in alone or in combinations on LPO, ROS, and ΔΨm 48 h of post-exposure on bMSCs. Each column represents Mean ± SEM ($n = 6$), different superscripts differ significantly from each other ($p \leq 0.05$) in One-way ANOVA with Tukey's multiple comparison *post hoc* test. CBZ: carbendazim, IMI: imidacloprid, ROS: reactive oxygen species, ΔΨm: mitochondrial membrane potential.

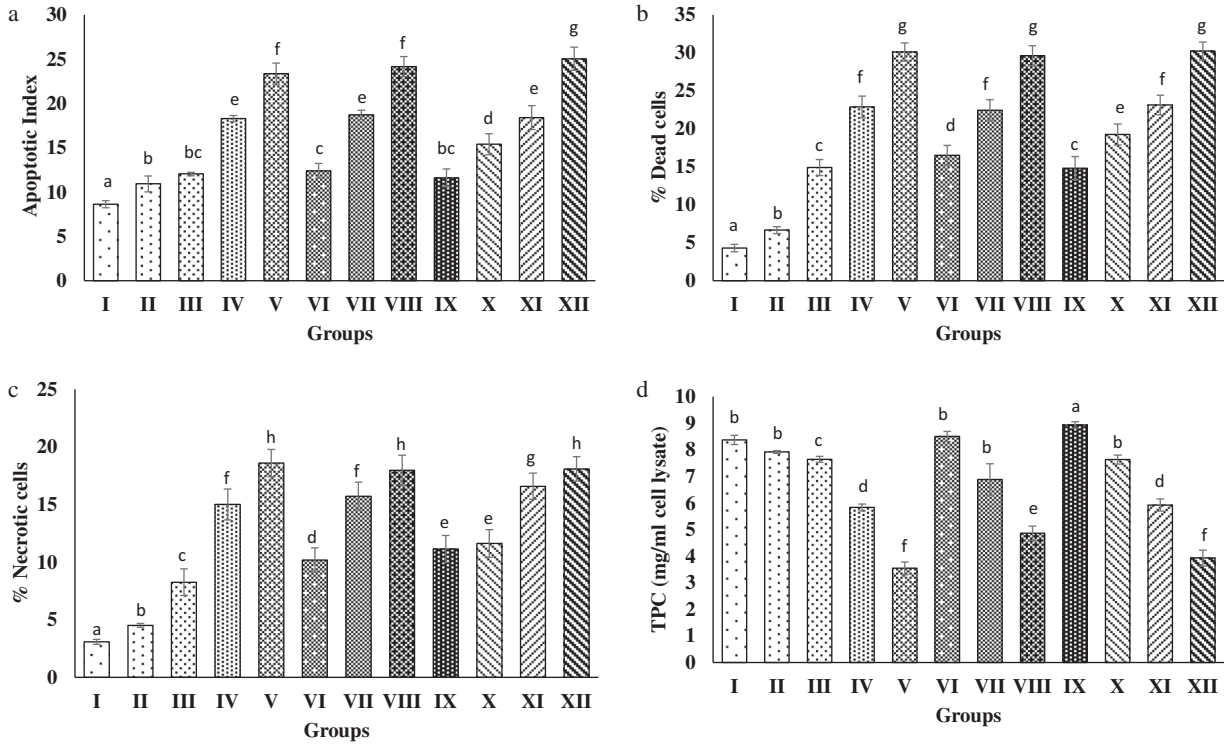

Figure 8. Effect of CBZ and IMI alone or in combinations on apoptotic indicators after 48 h of post-exposure on bMSCs. Each column represents Mean ± SEM ($n = 6$), different superscripts differ significantly from each other ($p \leq 0.05$) in One-way ANOVA with Tukey's multiple comparison *post hoc* test. CBZ: carbendazim, IMI: imidacloprid.

compared to the control group (Figure 10). CBZ-III treated group showed significant change ($p < 0.05$) in tail length, tail DNA percent, tail moment, and olive moment as compared to IMI alone treatment groups.

Effect of combinations/interaction index

The values of the joint effect of the binary mixture are expressed as an interaction index for different

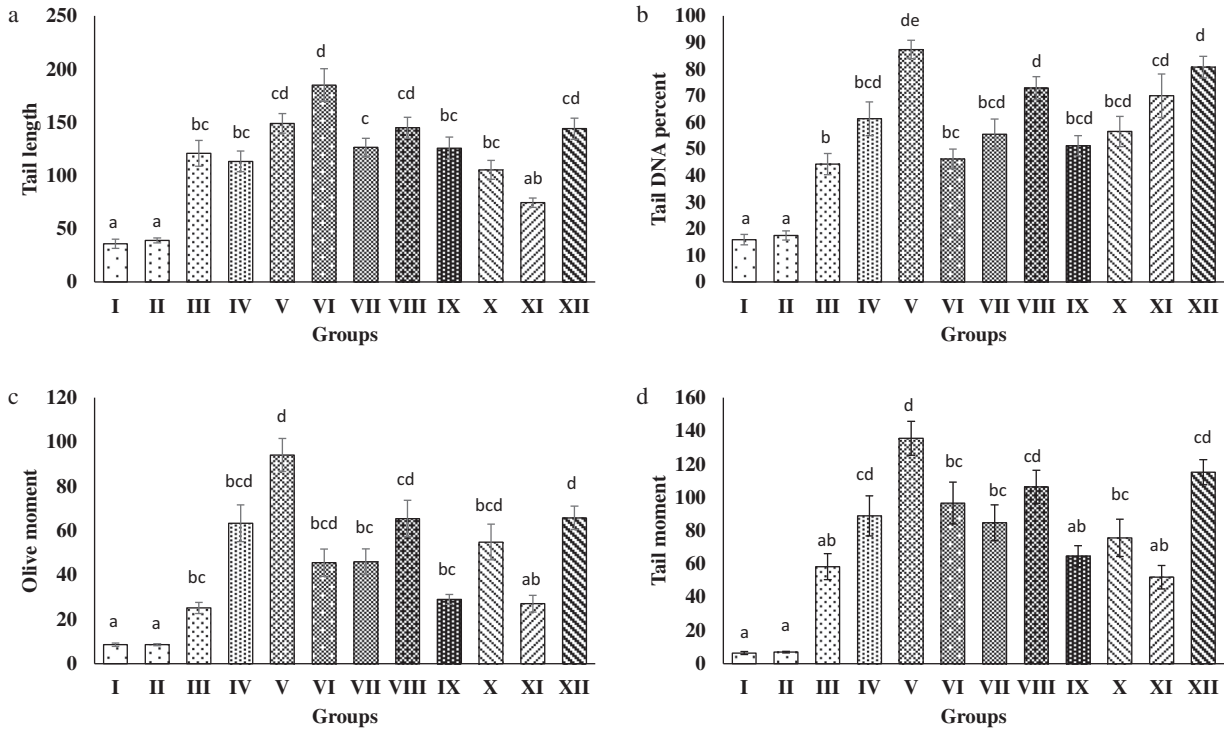

Figure 9. Effect of CBZ and IMI alone or in combinations on comet parameters (tail length, DNA percent, olive moments, tail moment) 48 h of post-exposure on bMSCs. Each column represents Mean ± SEM ($n = 6$), different superscripts differ significantly from each other ($p \leq 0.05$) in One-way ANOVA with Tukey's multiple comparison *post hoc* test. CBZ: carbendazim, IMI: imidacloprid.

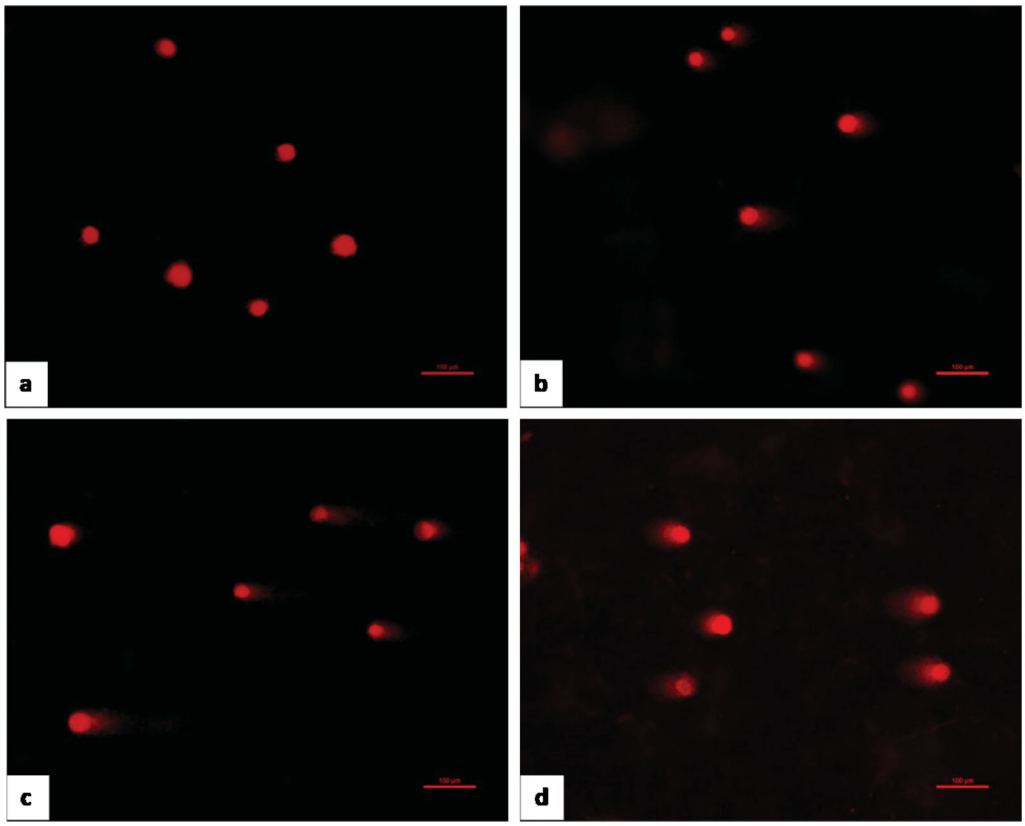

Figure 10. Photomicrographs of a selected comet showing DNA damage in bMSCs after completion of exposure time. (a) Normal cells with no DNA damage & (b–d) low, moderate, and a high degree of DNA damage indicated by tail length (Original magnification: (a–d): X20).

biochemical and genotoxicity parameters. The interactive index was calculated for 16 parameters (Tables 4, 5 and Figure 11). CBZ-I plus IMI-I and CBZ-I plus IMI-II combination groups showed the highest number of antagonism in parameters studied, while, CBZ-II plus IMI-I combination group showed 50% antagonism. Interestingly,

CBZ-II plus IMI-II combination showed more potentiation than the antagonism.

Discussion

The bMSCs with positive alkaline phosphatase activity appeared red after staining indicating that the cells were in a healthy, actively growing state and phenotypically undifferentiated condition. Similar findings have been reported for caprine mesenchymal stem cells derived from fetal tissue which were found positive for alkaline phosphatase activity in third passage cells (Somal *et al*. 2016). The bMSCs also showed positive expression of stem cell markers, CD73 and OCT4, as revealed by green and red fluorescence, respectively, indicating that bMSCs possessed progenitor and pluripotency properties. In support of our observation, similar results of expression of stem cell markers, CD73 and OCT4, in bone marrow-derived MSCs and amniotic mesenchymal stem cells of buffalo origin have been reported (Gade *et al*. 2012, Devi *et al*. 2017, Deng *et al*. 2018).

In the present study, IC_{50} value of IMI was found to be very high (6.446 mM) as compared to the IC_{50} value of CBZ (17.97 μM) indicating that CBZ is more toxic to bMSCs. These findings are incongruity with an *in vivo* study which showed that the lethal dose (LD_{50}) of IMI was less than that of CBZ. IMI is metabolized by liver isoenzymes and the nitrosoguanidine (C = N-NO) metabolite of IMI has moderate to high insecticidal activity through nAChR, whereas, the guanidine (C = NH) metabolite is highly active against mammalian nAChR and is more toxic to the mammalian system (Tomizawa *et al*. 2000). The absence of a metabolic enzyme system and nAChR under *in vitro* conditions might be responsible for the higher value of IMI required for producing its effect on bMSCs. It may require a greater concentration to produce its toxic effect by other mechanisms, which was reflected by a higher IC_{50} value of IMI than CBZ.

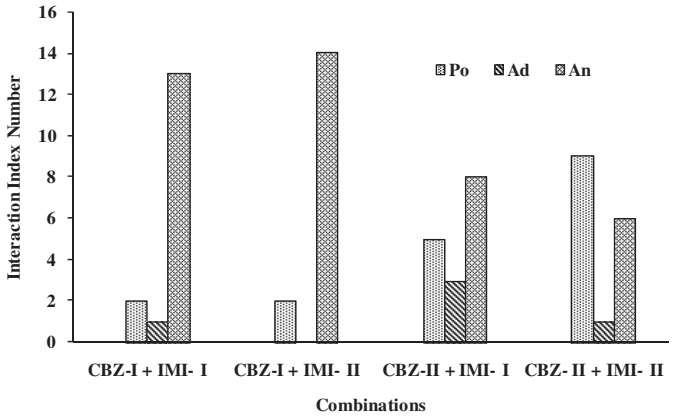

Figure 11. A number of parameters showing the interaction index expressed numerically corresponding to the joint action. Where, IMI: Imidacloprid, CBZ: Carbendazim, Po: Potentiation, Ad: Additive, An: Antagonistic, I.I.: Interactive index.

The morphological changes such as vacuolization of cytoplasm, cell shrinkage, diverse degrees of chromatin condensation, and cell membrane destruction along with dissolution in higher doses treatment groups were observed. A decrease in cell viability percentage and an increase in LDH values with a varying degree was noticed in bMSCs exposed to CBZ and IMI alone as well as in combination treatments. Change in viability and LDH release was significant in pesticide treatments as compared to the control group. This may be due to an alteration in the gene expression and cell apoptosis in the pesticide-exposed cells, which was responsible for cell damage and death. A very low dose of CBZ and IMI alone or in combination had very little or no toxic effect on cellular biochemicals studied and the cells remained unaffected in their presence. LDH activity has been suggested as an indicator of cytotoxicity which has a direct correlation with cell damage and viability. Pesticide exposure results in cellular damage, which leads to LDH leakage into the medium thus causing a decrease in cell viability (Jose *et al*. 2011). Similarly, reduction in cell viability in a dose-dependent pattern with CBZ-exposed human trophoblast cells (Adedara *et al*. 2013) and IMI-exposed human peripheral blood lymphocytes (Segura et al. 2012) has been reported. An increase in LDH level in the media, due to cellular damage, has also been reported after exposure to either a single pesticide or combinations of endrin, chlordane, alachlor, chlorpyrifos or fenthion (Chakroun *et al*. 2017) and imazalil, cypermethrin, and CBZ

Table 4. Interaction Index calculated on different antioxidants and cytotoxicity enzymes expressed by numerical values corresponding to the joint action.

Treatments (Concentrations)		GSH (no)	SOD (−)	CAT (−)	GPx (−)	GST (−)	TPC (−)	ALP (+)	CKMB (+)	GGT (+)
CBZ-I + IMI-I	2.25 μM + 0.81 mM	0.99^{po}	1.07^{an}	1.12^{an}	1.18^{an}	0.95^{po}	1.07^{an}	1.00^{ad}	0.94^{an}	0.97^{an}
CBZ-I + IMI-II	2.25 μM + 1.61 mM	0.96^{po}	1.08^{an}	1.14^{an}	1.40^{an}	0.96^{po}	1.10^{an}	0.96^{an}	0.74^{an}	0.96^{an}
CBZ-II + IMI-I	4.49 μM + 0.81 mM	1.03^{an}	0.96^{po}	1.10^{an}	1.28^{an}	0.94^{po}	1.00^{ad}	1.02^{po}	1.05^{po}	0.99^{an}
CBZ-II + IMI-II	4.49 μM + 1.61 mM	1.00^{ad}	0.96^{po}	1.04^{an}	1.92^{an}	0.93^{po}	0.97^{po}	1.03^{po}	1.17^{po}	1.01^{po}

Superscripts; an = Antagonism; ad = Additive; po = Potentiation. Positive (+) and negative (−) signs are indicative of the effect of individual drugs on particular parameters with respect to control values as per the formula (Mansour and Refaie 2000).

Table 5. Interaction Index calculated on different oxidative stress and genotoxicity indicators expressed by numerical values corresponding to the joint action.

Treatments (Concentrations)		LPO (+)	LDH (+)	Viability (−)	O^{2-} radicals (+)	ROS (% cells) (+)	ΔΨm (% cells) (+)	Tail moment (+)
CBZ-I + IMI-I	2.25 μM + 0.81 mM	0.90^{an}	0.99^{an}	1.09^{an}	0.94^{an}	0.38^{an}	0.46^{an}	0.42^{an}
CBZ-I + IMI-II	2.25 μM + 1.61 mM	0.84^{an}	0.97^{an}	1.09^{an}	0.91^{an}	0.34^{an}	0.57^{an}	0.37^{an}
CBZ-II + IMI-I	4.49 μM + 0.81 mM	1.00^{ad}	0.99^{an}	1.00^{ad}	1.02^{po}	0.45^{an}	0.31^{an}	0.49^{an}
CBZ-II + IMI-II	4.49 μM + 1.61 mM	1.09^{po}	1.01^{po}	1.02^{an}	1.22^{po}	0.55^{an}	0.70^{an}	0.56^{an}

Superscripts; an = Antagonism; ad = Additive; po = Potentiation. Positive (+) and negative (−) signs are indicative of the effect of individual drugs on particular parameters with respect to control values as per the formula (Mansour and Refaie 2000).

(Dikic *et al*. 2011). Further, a synergistic effect on decline in the cell viability was observed when human keratinocyte cells were exposed to the mixture of pesticides alpha-hexachlorocyclohexane, parathion methyl, and carbofuran (Abhishek 2014).

An increase in the cytotoxicity indicator enzyme levels in CBZ and IMI alone and in low dose combination groups, observed in the present study, were similar to previous reports of animal studies on CBZ and IMI treatments (Zaahkook *et al*. 2009, Waghe *et al*. 2013). Present findings are in agreement with the report that showed insecticide and fungicide combinations to be synergistic (Ilboudo *et al*. 2014). Further, an increase in the level of LDH, AST, ALT, GGT, ALP, creatinine, and albumin has been shown in CBZ-treated goats (Waghe *et al*. 2013), and IMI-treated rats (Arfat *et al*. 2014, Chakroun *et al*. 2017). ALP, LDH, and CK are usually involved in cell membrane integrity. The cellular damage caused by toxicants may have resulted in the alteration in the activity of these enzymes. Leakage of enzymes from the injured cells into the medium is widely used as a biochemical marker for loss of cellularity, cytotoxicity or cell death (Kopperschlager & Kirchberger 1996).

Total protein content has a direct correlation with toxicity caused by the toxicants. Thus, the measurement of total protein content acts as a promising tool for the detection of the changes caused by the toxicants and their nature under the *in vitro* and *in vivo* systems (Mansour and Mossa 2010, Costa *et al*. 2011). A non-significant, dose-dependent decrease in the protein content following exposure to the low dose of a single pesticide or low dose combinations was noticed in the present study. This could be due to the breakdown of cell membrane proteins responsible for the cellular loss after being exposed to CBZ and IMI (Teimouri *et al*. 2006) and the low concentration of pesticides may not have been sufficient to oxidize the cellular proteins and cause cell membrane damage. Present findings are in agreement with the report in which the decrease in the TPC was observed in different tissues when exposed to pesticides (Cetin *et al*. 2010, Lonare *et al*. 2017). Protein oxidation can induce several processes including metal-catalyzed oxidation, oxidation-induced cleavage, amino acid oxidation, and the conjugation of lipid peroxidation products (Berlett and Stadtman 1997). Further, oxidized proteins form aggregates may have an inhibitory effect on the functional enzymatic activity responsible for their degradation, which in turn, promotes the accumulation of modified proteins in cells and may even result in cell death (Grune and Davies 2003).

Lipid peroxidation of the inner mitochondrial membrane reduces the electric potential and energy generation, which accelerates the aging process by a defective DNA repair system (Pan *et al*. 2016). Cell viability gets affected due to the change in $\Delta\Psi$m under various stress conditions (Zorova *et al*. 2018) and plays an important role in pathological conditions such as cancer, cardiovascular diseases, diabetes, and neurodegenerative diseases (Pieczenik and Neustadt 2007). $\Delta\Psi$m is directly or indirectly involved in heat generation, control of redox and pH microenvironments, cell homeostasis, proliferation, ROS generation, membrane pore stabilization, maintenance of other signaling pathways, and cell death. Induction of amnion cell senescence via a mechanism involving ROS and DNA damage along with activation of ASK1, P-p38 MAPK, and p19Arf has been noticed after exposure to several toxicants (Menon *et al*. 2013). These reports support the findings of the present study, where an increase in the level of ROS, loss of $\Delta\Psi$m, and increased apoptotic index were noticed in cells exposed to either CBZ and IMI alone or in combinations. A decrease in the $\Delta\Psi$m and ROS production may have an influence on the process of apoptosis and cell death or viability (Lemasters *et al*. 2002) which was observed in the present study. LPO and ROS in response to high concentrations of IMI and CBZ alone and low dose combinations were quite similar. The findings are in agreement with the reports of Ge *et al*. (2015), who stated that LPO is indicative of cell membrane damage and is connected with the generation of ROS content responsible for toxicity. The values of LPO and O_2^- radical following exposure to low doses of CBZ and IMI alone and their combination were found to be similar to the control group indicating that these doses had the least toxic effect on cell phospholipids and mitochondrial membrane responsible for less free radical (ROS and O_2^- radical) production.

In this study, it was observed that comparatively higher O_2^- radical production occurred in CBZ-treated bMSCs than that in IMI-exposed bMSCs. An increase in the LPO and ROS production in CBZ, IMI, and in the combination-treated groups, in a dose-dependent manner, was noticed. This indicated the depressed antioxidant status of bMSCs, which might be due to cell damage caused by excessive free radicals generated in the medium. It has been reported that fungicides are known to generate a high amount of ROS and cause oxidative stress in the exposed cells (Sakr and Shalaby 2014, Ge *et al*. 2015, Shahid *et al*. 2018). Generation of ROS and O_2^- radicals have been explained to cause oxidative stress when the production of radicals exceeds the level of synthesis of antioxidants which leads to cellular damage and resultant pathological state (Livingstone 2001, Gulcin 2002). ROS generation is involved in the toxicological events mediated by pesticides (cypermethrin and/or chlorpyrifos) such as induction of chromosomal aberrations, micronuclei formation, cell proliferation inhibition, DNA damage, and apoptosis (Chauhan *et al*. 2016, Badgujar *et al*. 2017, Bano and Mohanty 2020).

Comet assay is a genotoxicity testing method, widely applied to detect DNA damage induced by toxicants in mammalian cells. The effects of various toxic agents on oxygen-radical-generated DNA damage in mammalian isolated cells have been investigated by this assay (Lee *et al*. 2004, Pandir 2015). DNA is the critical target for lethal, carcinogenic, teratogenic, and mutagenic effects of environmental toxicants. Initially, tail lengths were considered to be an index of DNA damage (Olive *et al*. 1990, Tice *et al*. 2000) but the subsequent introduction of computerized image analysis added more features to the comet assay such as tail length, tail moment, and olive moment. This provides a more clear picture of the overall DNA damage inside the cells (Olive *et al*. 1990). The tail moment (product of the tail length and the tail intensity) has been considered as the standard index of toxicant-induced DNA damage. It is indicative of both the

amount of DNA damaged and the distance of migration of the chromosomal material in the form of the tail (Vaghef and Hellman 1995). The olive tail moment is useful in describing heterogeneity within a cell population and variations in DNA distribution within the tail (Olive *et al*. 1990). The amount of DNA present and the distance of migration indicate the number of strand breaks within a cell which is reflected in form of tail or appears as a comet. The greater the migration of the chromosomal DNA from the nucleus, the higher will be the level of DNA damage (Rahman *et al*. 2002, Pandir 2015). In the present study, it was noticed that CBZ and IMI treated bMSCs showed a significant increase in tail length, tail moment, and olive moment with tail DNA content. This indicated significant chromosomal breakage within bMSCs after exposure to IMI or CBZ alone and in combinations. This increase in tail length might be due to ROS production caused by CBZ and IMI which was responsible for oxidative damage (Sakr and Shalaby 2014, Ge *et al*. 2015, Shahid *et al*. 2018). ROS may have caused the change in MTP and cell membrane damage leading to apoptosis and chromosomal DNA breakage which appeared in the form of the comet tail. Comet tail showed uniform distribution of fragmented DNA with variable length in the form of a single comet. In support of the present findings, exposure to pesticide-induced chromosomal damage and, micronuclei formation along with apoptotic changes has been reported by many workers (Chauhan *et al*. 2016).

A mixture can be defined as a combination of two or more environmental agents (Groten *et al*. 2001, Sexton and Hattis 2007). The generated and co-incidental mixtures created in the environment are countless and their impact on human health is largely unknown. Interactions may take place in the toxicokinetic phase and/or in the toxicodynamic phase, which may be weaker (antagonistic) or stronger (potentiated or synergistic). The data of generalized and biochemical findings of the present study revealed that the mixture comprising of a fungicide and an insecticide affected the activity of the concerned enzymes, where lower combinations showed antagonism while high-dose combinations showed potentiation. The combination of IMI and CBZ treatment showed a less prominent effect on the parameters studied as compared to the sum of their individual effects, indicating that the predominant antagonistic effect was in a similar pattern as that of earlier reports on pesticides studies (Krishnan *et al*. 1994, Mansour *et al*. 2001). Agent-to-agent interactions, toxicokinetic and toxicodynamic interactions (Viau 2002, Mumtaz *et al*. 2007, Sexton and Hattis 2007) have been described by a mathematical model to predict the type of toxicity of mixtures. Moreover, toxicity is not always simple to predict for mixtures because interaction may be influenced by the dose and the dose ratio, common cellular targets or metabolic pathways (Rashatwar and Matsumura 1985, Spurgeon *et al*. 2010).

Combined exposure to several pesticides has been shown to result in greater ROS and LPO as an indicator of oxidative stress (Banerjee *et al*. 2001, Halliwell & Gutteridge 2007, Mansour and Mossa 2010). A similar pattern was noticed with a high dose of CBZ and IMI exposure alone and in combination in the present study. Potentiation or synergistic effect on ROS production, genotoxicity, and cell cytotoxicity has been reported on human keratinocyte cells when exposed to combinations of alpha-hexachlorocyclohexane, parathion, and carbofuran mixture as compared to the effect on exposure to a single pesticide (Abhishek *et al*. 2014). CBZ, when combined with imazalil or cypermethrin, exhibited a more toxic effect on hepatocytes (Dikic *et al*. 2011, Wei *et al*. 2016, Cevik *et al*. 2017), on germ cells and sperm motility when combined with iprodione (Pisani *et al*. 2016), and on DNA damage when combined with triclosan (Silva *et al*. 2015). In the present study, a low-dose combination of CBZ and IMI was shown to be antagonistic on ROS, DNA damage, and apoptosis indicating weaker interaction at lower dose combinations. In contrast, a high-dose combination of CBZ and IMI resulted in a potentiating or synergistic effect, indicating stronger interaction at a high-dose combination.

The majority of *in vitro* toxicological research work is typically carried out using transform or immortalized cell lines. These cells are readily available and can easily be maintained but they usually show anomalous behavior and phenotypes, which do not reflect exactly the mechanisms observed in their normal homologous cells. The successful utilization of bMSCs in the present study for the predicting toxicological response of drug-drug interaction suggests that isolated bMSCs of buffaloes may represent a very good promising tool for the development of *in vitro* assays over commercial cell lines. This may ultimately replace and improve the future approach of predictive toxicological research on targeted animal species.

5. Conclusion

The present study represents the first evidence of the utilization of buffalo mesenchymal stem cells derived from bone marrow for the multi-chemical (CBZ and IMI) toxicological assessment and elaborates the potential mechanisms of toxicants. Present findings suggest that CBZ and IMI-induced toxicity in bMSCs is mediated via ROS production, $\Delta\Psi m$, LPO, and lower antioxidant status responsible for apoptosis and cell damage. However, the co-existence of CBZ and IMI at high doses had a pronounced potentiating effect on oxidative stress, cytotoxicity, and apoptosis, while low dose combinations failed to induce biochemical alterations indicating antagonism or weak interaction. This study gathered essential knowledge on the toxic effects caused by CBZ and IMI on bMSCs either alone or in combination. Further investigations are needed to evaluate the effect of low-dose, long-time exposure alone and in combinations of CBZ and IMI on toxicological indicators such as DNA damage, apoptosis, cell senescence, stem cell differentiation, proliferation, and gene expression on bMSCs; this will greatly contribute to the risk evaluation in animals and humans.

Acknowledgements

The authors would like to thank the Director of Research and Dean Postgraduate Studies, Guru Angad Dev Veterinary and Animal Sciences University, Ludhiana, Punjab, India for financial assistance and providing institutional facilities. The authors fully acknowledge Dr. Sidharth

Deshmukh, Assistant Pathologist for his assistance in fluorescence microscopy and all other scientific staff of Guru Angad Dev Veterinary and Animal Sciences University, Ludhiana who helped directly or indirectly in the completion of the study.

Disclosure statement

The authors do not have any competing potential interests that may bias the findings of this study in any manner.

Funding

The author(s) reported there is no funding associated with the work featured in this article.

References

Abhishek, A., *et al.*, 2014. *In vitro* toxicity evaluation of low doses of pesticides in individual and mixed condition on human keratinocyte cell line. *Bioinformation*, 10 (12), 716–720.

Adedara, I.A., *et al.*, 2013. Kolaviron prevents carbendazim-induced steroidogenic dysfunction and apoptosis in testes of rats. *Environmental Toxicology and Pharmacology*, 35 (3), 444–453.

Aebi, H., 1984. Catalase in vitro. *Methods in Enzymology*, 105, 121–126.

Aranda, A., *et al.*, 2013. Dichloro-dihydro-fluorescein diacetate (DCFH-DA) assay: a quantitative method for oxidative stress assessment of nanoparticle-treated cells. *Toxicology in Vitro*, 27 (2), 954–963.

Arfat, Y., *et al.*, 2014. Effect of imidacloprid on hepatotoxicity and nephrotoxicity in male albino mice. *Toxicology Reports*, 1, 554–561.

Badgujar, P.C., *et al.*, 2017. Fipronil-induced genotoxicity and DNA damage *in vivo*: protective effect of vitamin E. *Human & Experimental Toxicology*, 36 (5), 508–519.

Bahuguna, A., *et al.*, 2017. MTT assay to evaluate the cytotoxic potential of a drug. *Bangladesh Journal of Pharmacology*, 12 (2), 8–18.

Banerjee, B.D., Seth, V., and Ahmed, R.S., 2001. Pesticide-induced oxidative stress: perspectives and trends. *Reviews on Environmental Health*, 16 (1), 1–40.

Bano, F., and Mohanty, B., 2020. Thyroid disrupting pesticides mancozeb and fipronil in mixture caused oxidative damage and genotoxicity in lymphoid organs of mice. *Environmental Toxicology and Pharmacology*, 79, 103408.

Baskić, D., *et al.*, 2006. Analysis of cycloheximide-induced apoptosis in human leukocytes: fluorescence microscopy using annexin V/propidium iodide versus acridin orange/ethidium bromide. *Cell Biology International*, 30 (11), 924–932.

Berlett, B.S., and Stadtman, E.R., 1997. Protein oxidation in aging, disease, and oxidative stress. *Journal of Biological Chemistry*, 272 (33), 20313–20316.

Beutler, E., and Kelly, B.M., 1963. The effect of sodium nitrite on red cell GSH. *Experientia*, 19, 96–97.

Bind, V., and Kumar, A., 2019. Pesticides toxicity may causes adverse effects to our health- a review. *MOJ Toxicology*, 5 (1), 17–18.

Caron-Beaudoin, E., *et al.*, 2017. The use of a unique co-culture model of fetoplacental steroidogenesis as a screening tool for endocrine disruptors: the effects of neonicotinoids on aromatase activity and hormone production. *Toxicology and Applied Pharmacology*, 332, 15–24.

Cetin, E., *et al.*, 2010. Propetamphos-induced changes in haematological and biochemical parameters of female rats: protective role of propolis. *Food and Chemical Toxicology*, 48 (7), 1806–1810.

Cevik, U., *et al.*, 2017. Antiproliferative, cytotoxic, and apoptotic effects of new benzimidazole derivatives bearing hydrazone moiety. *Journal of Heterocyclic Chemistry*, 55 (1), 138–148.

Chakroun, I.G., *et al.*, 2017. Imidacloprid enhances liver damage in wistar rats: biochemical, oxidative damage and histological assessment. *Journal of Coastal Life Medicine*, 5 (12), 540–546.

Chauhan, L.K., *et al.*, 2016. Reactive oxygen species-dependent genotoxicity, cell cycle perturbations and apoptosis in mouse bone marrow cells exposed to formulated mixture of cypermethrin and chlorpyrifos. *Mutagenesis*, 31 (6), 635–642.

Costa, R.N., *et al.*, 2011. A Reassessment of the *in vitro* total protein content determination (tpc) with sirc and 3t3 cells for the evaluation of the ocular irritation potential of shampoos: comparison with the *in vivo* draize rabbit test. *Brazilian Archives of Biology and Technology*, 54 (6), 1135–1145.

Damalas, C., and Koutroubas, S., 2017. Farmers training on pesticide use is associated with elevated safety behavior. *Toxics*, 5 (3), 19.

Deng, Y., *et al.*, 2018. Isolation and characterization of buffalo (bubalus bubalis) amniotic mesenchymal stem cells derived from amnion from the first trimester pregnancy. *The Journal of Veterinary Medical Science*, 80 (4), 710–719.

Devi, P., *et al.*, 2017. Viability and expression pattern of cryopreserved mesenchymal stem cells derived from buffalo bone marrow. *Ruminant Science*, 6 (1), 7–12.

Dikic, D., *et al.*, 2011. Carbendazim combined with imazalil or cypermethrin potentiate DNA damage in hepatocytes of mice. *Human and Experimental Toxicology*, 31 (5), 492–505.

Gade, N.E., *et al.*, 2012. Molecular and cellular characterization of buffalo bone marrow-derived mesenchymal stem cells. *Reproduction in Domestic Animals*, 48 (3), 358–367.

Ge, W., *et al.*, 2015. Oxidative stress and DNA damage induced by imidacloprid in zebrafish (Danio rerio)). *Journal of Agricultural and Food Chemistry*, 63 (6), 1856–1862.

Gilliom, R. J., *et al.*, 2006. Pesticides in the nation's streams and ground water, 1992–2001: U.S. Geological Survey Circular 1291, The Quality of Our Nation's Waters, 184. https://pubs.er.usgs.gov/publication/cir1291.

Groten, J.P., Feron, V.J., and Sühnel, J., 2001. Toxicology of simple and complex mixtures. *Trends in Pharmacological Sciences*, 22 (6), 316–322.

Grune, T., and Davies, K.J., 2003. The proteasomal system and HNE-modified proteins. *Molecular Aspects of Medicine*, 24 (4–5), 195–204.

Gulcin, I., 2002. Determination of antioxidant activity of Lichen cetrariaislandica (L) Ach. *Journal of Ethnopharmacology*, 79, 325–329.

Habig, W.H., Pabst, M.J., and Jakoby, W.B., 1974. Glutathione S-transferases the first enzymatic step in mercapturic acid formation. *Journal of Biological Chemistry*, 249 (22), 7130–7139.

Hafeman, D.G., Sunde, R.A., and Hoekstra, W.G., 1974. Effect of dietary selenium on erythrocyte and liver glutathione peroxidase in the rat. *The Journal of Nutrition*, 104 (5), 580–587.

Halliwell, B., and Gutteridge, J. M. C., 2007. *Free Radicals in Biology and Medicine (4th Edn)*. New York: Oxford University Press, 704.

Hernández, A.F., Gil, F., and Lacasaña, M., 2017. Toxicological interactions of pesticide mixtures: an update. *Archives of Toxicology*, 91 (10), 3211–3223.

Ilboudo, S., *et al.*, 2014. *In vitro* impact of five pesticides alone or in combination on human intestinal cell line Caco-2. *Toxicology Reports*, 1, 474–489.

Jose, S., *et al.*, 2011. Application of primary haemocyte culture of *Penaeus monodon* in the assessment of cytotoxicity and genotoxicity of heavy metals and pesticides. *Marine Environmental Research*, 71 (3), 169–177.

Kopperschlager, G., and Kirchberger, J., 1996. Methods for the separation of lactate dehydrogenases and clinical significance of the enzyme. *Journal of Chromatography B: Biomedical Sciences and Applications*, 684 (1-2), 25–49.

Krishnan, K., *et al.*, 1994., Physiologically based pharmacokinetic modeling of chemical mixtures. In: Yang, R.S.H. (Ed.), *Toxicology of chemical mixtures. Case studies, mechanisms and novel approaches*. San Diego, CA: Academic Press, 399–437.

Kumar, S., 2004. Occupational exposure associated with reproductive dysfunction. *Journal of Occupational Health*, 46 (1), 1–19.

Lee, E., *et al.*, 2004. Use of the tail moment of the lymphocytes to evaluate DNA damage in human biomonitoring studies. *Toxicological Sciences*, 81 (1), 121–132.

Lemasters, J.J., *et al.*, 2002. Role of mitochondrial inner membrane permeabilization in necrotic cell death, apoptosis, and autophagy. *Antioxidants & Redox Signaling*, 4 (5), 769–781.

Livingstone, D.R., 2001. Contaminant-stimulated reactive oxygen species production and oxidative damage in aquatic organisms. *Marine Pollution Bulletin*, 42 (8), 656–666.

Lonare, M.K., *et al.*, 2017. Cytotoxicity and oxidative stress alterations induced by aldrin in Balb/C 3t3 fibroblast cells. *Proceedings of the National Academy of Sciences, India Section B: Biological Sciences*, 87 (4), 1209–1216.

Lowry, H., *et al.*, 1951. Protein measurement with the Folin phenol reagent. *Journal of Biological Chemistry*, 193 (1), 265–275.

Madesh, M., and Balasubramanian, K.A., 1998. Microtiter plate assay for superoxide dismutase using MTT reduction by superoxide. *Indian Journal of Biochemistry & Biophysics*, 35 (3), 184–188.

Mansour, S.A., Refaie, A.A., and Nada, A.S., 2001. Xenobiotics interaction. 4. Effect of some pesticides and their mixtures on the growth rate of albino rats. *Advances in Pharmacology and Toxicology*, 2 (2), 9–24.

Mansour, S.A., and Refaie, A.A., 2000. Xenobiotics interaction 2. An approach to the use of biochemical data measurements interpreting interaction of insecticide the mixtures in rat. *Advances in Pharmacolology and Toxicolology*, 1 (1), 1–20.

Mansour, S.A., and Mossa, A.H., 2010. Oxidative damage, biochemical and histopathological alterations in rats exposed to chlorpyrifos and the antioxidant role of zinc. *Pesticide Biochemistry and Physiology*, 96 (1), 14–23.

Menon, R., *et al.*, 2013. Senescence of primary amniotic cells via oxidative DNA damage. *PLoS One*, 8 (12), e83416.

Mumtaz, M.M., Ruiz, P., and De Rosa, C.T., 2007. Toxicity assessment of unintentional exposure to multiple chemicals. *Toxicology and Applied Pharmacology*, 223 (2), 104–113.

Olive, P.L., Banáth, J.P., and Durand, R.E., 1990. Heterogeneity in radiation-induced DNA-damage and repair in tumor and normal cells measured using the 'comet' assay. *Radiation Research*, 122 (1), 86–94.

Pan, M.-R., *et al.*, 2016. Connecting the dots: from DNA damage and repair to aging. *International Journal of Molecular Sciences*, 17 (5), 685.

Pandir, D., 2015. Assessment of the DNA damage in human sperm and lymphocytes exposed to the carcinogen food contaminant furan with comet assay. *Brazilian Archives of Biology and Technology*, 58 (5), 773–780.

Patil, N., *et al.*, 2018. Hemato-biochemical alterations mediated by carbendazim exposure and protective effect of quercetin in male rats. *Toxicology International*, 25 (1), 7–18.

Pieczenik, S.R., and Neustadt, J., 2007. Mitochondrial dysfunction and molecular pathways of disease. *Experimental and Molecular Pathology*, 83 (1), 84–92.

Pisani, C., *et al.*, 2016. *Ex vivo* assessment of testicular toxicity induced by carbendazim and iprodione, alone or in a mixture. *ALTEX*, 33 (4), 393–413.

Rahman, M.F., *et al.*, 2002. Assessment of genotoxic effects of chloropyriphos and acephate by the comet assay in mice leucocytes. *Mutation Research/Genetic Toxicology and Environmental Mutagenesis*, 516 (1-2), 139–147.

Rashatwar, S.S., and Matsumura, F., 1985. Interaction of DDT and pyrethroids with calmodulin and its significance in the expression of enzyme activities of phosphodiesterase. *Biochemical Pharmacology*, 34 (10), 1689–1694.

Sakr, S.A., and Shalaby, S.Y., 2014. Carbendazim-induced testicular damage and oxidative stress in albino rats: ameliorative effect of licorice aqueous extract. *Toxicology and Industrial Health*, 30 (3), 259–267.

Salmon, E.D., *et al.*, 2013. A high-resolution multimode digital microscope system. *Methods in Cell Biology*, 114, 179–210.

Segura, M.E.C., *et al.*, 2012. Evaluation of genotoxic and cytotoxic effects in human peripheral blood lymphocytes exposed *in vitro* to neonicotinoid insecticides news. *Journal of Toxicology*, 2012:612647.

Sexton, K., and Hattis, D., 2007. Assessing cumulative health risks from exposure to environmental mixtures – three fundamental questions. *Environmental Health Perspectives*, 115 (5), 825–832.

Shahid, M., *et al.*, 2018. Toxicity of fungicides to Pisumsativum: a study of oxidative damage, growth suppression, cellular death and morpho-anatomical changes. *RSC Advances*, 8 (67), 38483–38498.

Silva, A.R.R., *et al.*, 2015. Ecotoxicity and genotoxicity of a binary combination of triclosan and carbendazim to *Daphnia magna*. *Ecotoxicology and Environmental Safety*, 115, 279–290.

Somal, A., *et al.*, 2016. A comparative study of growth kinetics, *in vitro* differentiation potential and molecular characterization of fetal adnexa derived caprine mesenchymal stem cells. *PLoS One*, 11 (6), e0156821.

Stocks, J., and Dormandy, T.L., 1971. The autoxidation of human red cell lipids induced by hydrogen peroxide. *British Journal of Haematology*, 20 (1), 95–111.

Teimouri, F., *et al.*, 2006. Alteration of hepatic cells glucose metabolism as a non-cholinergic detoxication mechanism in counteracting diazinon-induced oxidative stress. *Human & Experimental Toxicology*, 25 (12), 697–703.

Tice, R.R., *et al.*, 2000. Single cell gel/comet assay: guidelines for *in vitro* and *in vivo* genetic toxicology testing. *Environmental and Molecular Mutagenesis*, 35 (3), 206–221.

Tomizawa, M., Lee, D.L., and Casida, J.E., 2000. Neonicotinoid insecticides: molecular features conferring selectivity for insect versus mammalian nicotinic receptors. *Journal of Agricultural and Food Chemistry*, 48 (12), 6016–6024.

Vaghef, H., and Hellman, B., 1995. Demonstration of chlorobenzene-induced DNA damage in mouse lymphocytes using the single cell gel electrophoresis assay. *Toxicology*, 96 (1), 19–28.

Valavanidis, A., *et al.*, 2006. Molecular biomarkers of oxidative stress in aquatic organisms in relation to toxic environmental pollutants. *Ecotoxicology and Environmental Safety*, 64 (2), 178–189.

Viau, C., 2002. Biological monitoring of exposure to mixtures. *Toxicology Letters*, 134 (1-3), 9–16.

Waghe, P., *et al.*, 2013. Sub-chronic exposure to carbendazim induces biochemical and hematological alterations in male goats. *Toxicological & Environmental Chemistry*, 95 (2), 330–336.

Wang, X., Kanel, G.C., and DeLeve, L.D., 2000. Support of sinusoidal endothelial cell glutathione prevents hepatic veno-occlusive disease in the rat. *Hepatology*, 31 (2), 428–434.

Wei, K.-L., *et al.*, 2016. Activation of aryl hydrocarbon receptor reduces carbendazim-induced cell death. *Toxicology and Applied Pharmacology*, 306, 86–97.

Zaahkook, S.A., *et al.*, 2009. Physiological study about imidacloprid toxicity and the role of vitamin C as a protective agent on Japanese Quails. *Egyptian Journal of Hospital Medicine*, 34, 183–197.

Zorova, L.D., *et al.*, 2018. Mitochondrial membrane potential. *Analytical Biochemistry*, 552, 50–59.